Combined Contention and TDMA-Based Communication in Wireless Sensor Networks

Vicente Casares-Giner*, Patrick Wüchner†, Diego Pacheco-Paramo*, Hermann de Meer†
*Universitat Politècnica de València, Spain
Email: vcasares@dcom.upv.es, diegofelipe.pacheco@gmail.com
†Department of Informatics and Mathematics, University of Passau, Germany
Email: {patrick.wuechner, hermann.demeer}@uni-passau.de

***Abstract*—Wireless sensor networks usually consist of a large number of very small, energy-constrained sensor nodes. The nodes capture information from their immediate environment to send it to a destination node (sink) in a timely manner.**

This work proposes a combined contention and TDMA-based approach for load balancing and a discrete-time Markov model that allows to study the trade-off between energy consumption and transfer delay in clustered wireless sensor networks.

Our investigations show that the length of the TDMA frame needs to be configured close to the minimum that is capable of transferring the offered load for optimizing energy efficiency and minimizing the delay.

***Index Terms*—Wireless sensor networks, clustering, contention, TDMA, energy, delay, queueing theory, discrete-time Markov model**

I. Introduction

Energy saving in wireless sensor networks (WSNs) is critical. Only a small amount of energy is available to the small sensor nodes that compose the network, i.e., a restrained energy consumption significantly benefits the WSN's lifetime. To reduce energy consumption, those strategies are of special interest that activate the sensor node's transceiver only if data is to be transmitted or received.

In this work, it is assumed that the transceivers of the immobile nodes operate on a single frequency and in three different operation modes: Reception ($\mathcal{R}$), Transmission ($\mathcal{T}$), and Sleeping ($\mathcal{S}$). The energy consumption of each node heavily depends on the current mode of operation. Also the frequency of the mode transitions affects energy consumption.

A second aspect is medium access. Data transfer towards the sink has to be completed in a timely manner and an uncoordinated transmission of data could easily lead to collisions. Hence, some coordination between sensor nodes regarding their operation modes is necessary. This induces some additional delay (see, e.g., [1]).

In this paper, we propose a communication protocol for geographically clustered WSNs, i.e., our clustering is not explicitly based on (logical) connectivity information but mainly on the nodes' (physical) positions within a grid of hexagonal *cells*[1]. The protocol controls medium access based on a combination of contention and TDMA with spatial frequency reuse for low-traffic intra-cell and high-traffic inter-cell communication, respectively. The protocol aims at balancing the load between nodes that have the same distance from the sink. We additionally develop a discrete-time Markov model that allows to find suitable protocol parameters that optimize the trade-off between energy efficiency and delay.

The geographical clustering provides a regular topology of the cell heads, which are located close to the cells' center. This is a major advantage for finding an energy-efficient, conflict-free TDMA schedule for inter-cell communication. Since the resulting topology is known in advance, the slot allocation is static and can be defined at design time. This saves the network from calculating a near-optimum schedule during runtime in a centralized (see, e.g., [2], [3]) or decentralized (like DRAND [4, p. 111]) manner, and hence, promises less computation and/or communication overhead. The approach of [5] also achieves a static slot schedule. However, the schedule is defined at runtime during a setup period for tree construction and slot assignment. This period comprises the necessary communication and processing overhead. Also note that our work differs from hybrid CSMA/TDMA protocols, like Z-MAC (see, e.g., [4, Sect. 5.5.1]) which also needs to assign the TDMA slots to all nodes during a setup phase (using DRAND).

The work is organized as follows: Section II describes the WSN scenario. The proposed communication protocol is introduced in Sect. III. The system model presented in Sect. IV and the quantitative energy and delay measures introduced in Sect. V are the basis of the exemplary quantitative results shown and discussed in Sect. VI. Finally, conclusions end the work in Sect. VII.

II. WSN Scenario

We assume that the investigated WSN consists of a large number (hundreds) of sensor nodes. Since this renders infeasible deterministic deployment, we assume nodes being randomly and uniformly distributed in a two-dimensional area. Sensor nodes are homogeneous, i.e., they consist of identical hardware and software configuration. We do not require the sensors to possess a unique identification. Moreover, note that some node parameters (like position, current energy level, and sensor readings) differ between nodes and based on these parameters nodes might take different roles or decisions. We assume that nodes are immobile and know their real physical

[1]We refrain from using the term *cluster* here, since we use it to describe a set of cells in Sect. III-C and following.

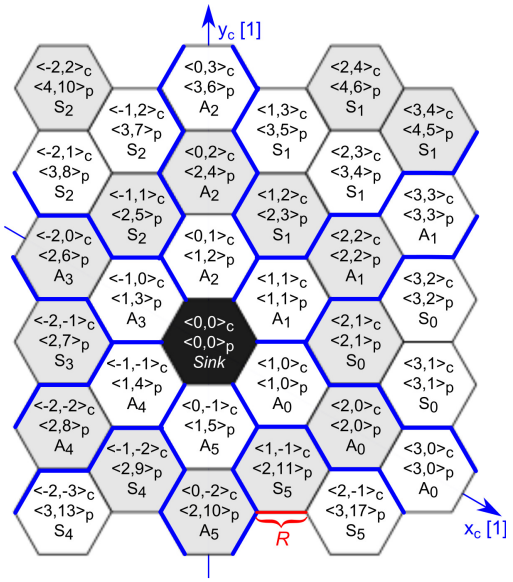

Fig. 1. Cell coordinates $\langle x, y\rangle_c$, polar coordinates $\langle r, m\rangle_p$, axes A_k and sectors S_k (R is the Cell Radius).

location in the area by applying some known localization technique (as surveyed in [6]–[8]). Moreover, all nodes are time-synchronized by using some synchronization method (see, e.g., [4, Ch. 11], [9]). Furthermore, we expect nodes' antennae to be omni-directional, and hence, their transmission ranges can be modeled as circles. The influence of obstacles on the radio ranges is considered negligible. There is only a single transceiver unit per node. Hence, the WSN operates on a single frequency.

A. Cells and Coordinates

For energy-efficient communication (see details in Sect. III), we divide the monitored area into cells, comparable to the approach presented in [10]. However, while the virtual grid formed in [10] is square with von Neumann neighborhood, we prefer a grid of hexagonal cells that approximates neighborhoods caused by circular transmission ranges more closely (cf. [11]). Each cell has the same size, defined by radius R (in meters) as depicted in Fig. 1. The value of R is a design parameter that depends on the node density and the nodes' intra-cell and inter-cell communication ranges. For the resulting hexagonal grid of cells, illustrated in Fig. 1, we introduce hexagonal coordinates in Cartesian-like form $\langle x, y\rangle_c$—in the following referred to as *cell coordinates*—such that the sink is located at the center of cell $\langle 0, 0\rangle_c$. For later convenience, we additionally introduce hexagonal coordinates in polar-like (or ring) form $\langle r, m\rangle_p$. We call these coordinates *polar coordinates* in the following. Finally, we introduce the notion of *axes* ($\pm 30, \pm 90, \pm 120$ degrees originating at sink) and *sectors* (cells between axes) and define them according to Table I. The transformation between the different coordinate systems is rather straightforward and not presented here due to space limitations.

TABLE I
DEFINITION OF AXES A_k AND SECTORS S_k, $0 \le k \le 5$.

Axis	Condition	Sector	Condition
A_0	$0 = y_h < x_h$	S_0	$0 < y_h < x_h$
A_1	$0 < y_h = x_h$	S_1	$0 < x_h < y_h$
A_2	$0 = x_h < y_h$	S_2	$x_h < 0 < y_h$
A_3	$x_h < y_h = 0$	S_3	$x_h < y_h < 0$
A_4	$x_h = y_h < 0$	S_4	$y_h < x_h < 0$
A_5	$y_h < x_h = 0$	S_5	$y_h < 0 < x_h$

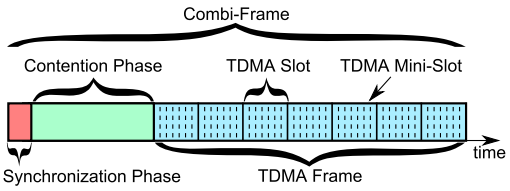

Fig. 2. Combi-frame structure.

III. COMMUNICATION

The member nodes of each cell elect a single cell head (CH) node. Head election algorithms are not the focus of this paper. The interested reader is referred to recent related work in this area (e.g., [12], [13], [14]) and the references therein. In the following, we assume for the sake of clarity that the node density is high enough such that every cell is able to find a CH which is close to the cell's center.

Communication is split into *intra-cell communication* (further detailed in Sect. III-B) and *inter-cell communication* (Sects. III-C and III-D). For each cell, the corresponding CH acts as a gateway between these two levels of communication. That is, intra-cell communication refers to the direct, i.e., single-hop communication between the CH and other cell members, and inter-cell communication refers to the communication from a source cell's CH to the sink, potentially in a multi-hop manner involving CHs of further inner-ring cells.

In both, intra-cell and inter-cell communications, the communication range needs to be high enough to guarantee the quality of the communication. According to [5], the interference ranges are at least twice the communication ranges. This fact must be considered when designing the corresponding MAC protocols in the combi-frame introduced in Sect. III-A.

A. Medium Access and Frame Structure

The potential interference of simultaneous intra-cell and inter-cell communication processes requires a concept of handling medium access. For this, we propose a combination of random-access contention for low-traffic intra-cell communication and TDMA for high-traffic inter-cell communication. The corresponding phases are combined to a so-called *combi-frame* (see Fig. 2). It starts with a short synchronization phase of fixed lengths T_{Syn} which is used to synchronize time of all nodes. For the sake of simplicity, let us assume that $T_{\text{Syn}} \approx 0$ and the influence of the synchronization phase on the network performance is negligible.

A contention phase of fixed lengths T_C follows. It is used for intra-cell communication according to some random-access

protocol. Since the number of nodes per cell is relatively small, we consider intra-cell traffic to be sparse enough to keep collision probability low (see Sect. III-B for more details).

However, this low-traffic assumption does not hold for inter-cell traffic. Hence, the remainder of the combi-frame comprises a TDMA frame which is used by the CHs to forward traffic to the sink. The TDMA frame consists of N_{TS} TDMA slots, each consisting of N_{MS} TDMA mini-slots of duration T_{MS}. We assume that in each single TDMA mini-slot exactly one data packet can be transmitted. Consequently, the TDMA slot duration is given by $T_{TS} = N_{MS} \cdot T_{MS}$, the TDMA frame duration is given by $T_{\text{TDMA}} = N_{TS} \cdot T_{TS}$, and the combi-frame duration is given by $T_{CF} = T_{\text{Syn}} + T_C + T_{\text{TDMA}} \approx T_C + T_{\text{TDMA}}$.

Based on its location and role, on the currently active phase of the combi-frame, and, if applicable, on the currently active slot in the TDMA frame, a node chooses to set its transceiver into one of three modes: Reception ($\mathcal{R}$), Sleeping ($\mathcal{S}$), and Transmission ($\mathcal{T}$). For example, during contention phase, all CHs are in mode $\mathcal{R}$ to receive data from other cell members while the latter switch to mode $\mathcal{T}$ in case of sensor data to be reported and to mode $\mathcal{S}$ otherwise. During TDMA phase, all non-head nodes switch to mode $\mathcal{S}$ and the CHs switch between $\mathcal{R}$, $\mathcal{S}$, and $\mathcal{T}$ according to a slot assignment scheme described in Sect. III-C.

B. Intra-Cell Communication during Contention Phase

During the contention phase, the cell members try to transmit data packets to their CH —using, e.g., a protocol of the slotted-ALOHA family (see [15]). For the sake of model simplicity, we assume a total of $N_{CS} = T_C / T_{MS}$ mini-slots—an integer number—in each contention phase. Only one data packet per mini-slot can be transmitted. Hence, there are $N_{FS} = N_{CS} + N_{TS} N_{MS}$ mini-slots in a combi-frame.

The value of N_{CS} influences the trade-off between intra-cell throughput and collisions on the one hand, and inter-cell throughput on the other hand. The value has to be selected in accordance to the communication protocol used for intra-cell communication during contention phase.

For example, clipped binary-tree collision resolution protocol with ternary feedback (cf. [15, Sect. 5.2.3]) achieve normalized throughputs up to approximately 0.5 (see, e.g., [16]), i.e., in the best-case scenario, the mean number of mini-slots successfully used in data packet transmissions is upper bounded by the approximately 50% of the allocated mini-slots. Consequently, *at least* two mini-slots should be foreseen for successful transmission of an arriving packet. We denote the number of mini-slots expected for a successful packet transmission by *contention factor* η, which is protocol-dependent. While for ideal multiplexing clearly we maintain that $\eta = 1$, for ALOHA and slotted ALOHA we should consider $\eta > 2e \approx 5.44$ and $\eta > e \approx 2.72$, respectively.

Note that in most collision resolution protocols, arriving packets are not considered for transmission until ongoing collisions are resolved (see [15, Ch. 5]). Therefore, we assume that packets that are generated by the cell members during a contention phase wait for transmission until the beginning of the next contention phase.

C. Inter-Cell Channel Reuse and TDMA Clusters

In order to avoid co-channel interference during inter-cell communication, we consider a channel reuse factor similar to cellular systems (see, e.g., [11]). That is, within a set (*cluster*) of CHs, the same TDMA transmission slot ($\mathcal{T}$-slot) can only be used by a single CH. Additionally, we specify that each CH gets exactly one $\mathcal{T}$-slot per TDMA frame. In all other $N_{TS} - 1$ slots, a CH is in mode $\mathcal{R}$ or $\mathcal{S}$. This implies that the number of TDMA slots per TDMA frame is equal to the number of CHs per cluster (called *cluster size* N_c), i.e., $N_{TS} = N_c$. Within a TDMA frame, we label the N_{TS} slots with consecutive numbers $0, 1, 2, \ldots, N_{TS} - 1$.

In general, choosing cluster size N_c and consequently frame length N_{TS} allows us to balance the trade-off between interference and network throughput. For example, a high N_c increases the distance between CHs that use the same $\mathcal{T}$-slot. On the other hand, higher N_c implies a longer TDMA frame, and hence, each CH experiences a longer interval between consecutive $\mathcal{T}$-slots, and consequently, a lower bandwidth.

Remember, however, that we assume interference only between cells that are up to two hops apart. Hence, a cluster size of $N_c = 12$ is sufficient in our scenario[2]

It can be shown that for $N_c = 12$, each CH can unambiguously derive its $\mathcal{T}$-slot ($T(\langle x, y \rangle_c) = (2x_c + 2y_c - y_c \bmod 2) \bmod 12$), based on its cell coordinates $\langle x, y \rangle_c$. Following this rule, all CHs of the same cluster use different $\mathcal{T}$-slots.

Note that a CH cannot receive packets from other nodes while it is in mode $\mathcal{T}$. Nevertheless, the node might receive data from its own sensor board anytime. We assume that packets that arrive to the CH during its $\mathcal{T}$-slot are deferred to be transmitted in upcoming $\mathcal{T}$-slots. This allows a sending node to switch from mode $\mathcal{T}$ to $\mathcal{S}$ as soon as its transmission buffer becomes empty. Analogously, the receiving node can switch from $\mathcal{R}$ to $\mathcal{S}$ as soon as it detects the first mini-slot without data. Both nodes can then stay in mode $\mathcal{S}$ at least until the end of the current TDMA slot. Consequently, the energy consumption of both nodes is reduced.

D. Inter-Cell Routing and Load Balancing

The inter-cell routing protocol used by all CHs boils down to transferring information to a neighboring cell's CH (called *neighbor* in the following) that is closer to the sink, i.e., from ring r to the next inner ring $r - 1$. Assuming full availability of all CHs, there is a minimum of one and a maximum of two inner-ring neighbors (see Fig. 1). To resolve this potential conflict of redundant receivers, for any CH $\langle x, y \rangle_c$, there needs to be exactly one single inner-ring neighbor that is in reception mode $\mathcal{R}$ in each time slot $T(x, y)$.

[2]The same slot reuse concept can be applied for intra-cell communication. But, due to low-power transmission, perhaps a reuse factor around 4 could be sufficient in this case.

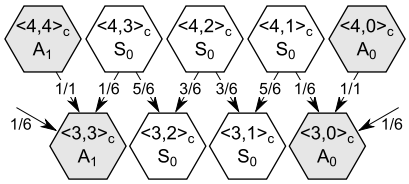

Fig. 3. Load balancing from ring 4 to ring 3 in sector S_0.

Moreover, to assure that all CHs of the same ring handle the same traffic load, the percentages of receptions by potential receivers need to be balanced suitably. In other words, assuming that the overall traffic load in ring $r+1$ is evenly distributed on all CHs in ring $r+1$, we want to transfer this traffic load to the CHs in ring r in such a way that it is again evenly distributed. Then, each CH in ring r has to cope with $1+1/r$ times the per-CH load of ring $r+1$ — plus the load originating from r itself.

Consider the example presented in Fig. 3, which shows an extract of sector S_0 for rings $3 \le r \le 4$ and the adjacent axes' cells. Every CH in ring 3 needs to take care of $1+1/3$ times the per-CH load of ring 4. For example, since CH $\langle 3,3\rangle_c$ is the only inner-ring neighbor of CH $\langle 4,4\rangle_c$, it needs to be in mode $\mathcal{R}$ each time CH $\langle 4,4\rangle_c$ transmits. Therefore, CH $\langle 3,3\rangle_c$ must be in mode $\mathcal{R}$ in slot $T(\langle 4,4\rangle_c)$ of each TDMA frame. On the other hand, CHs $\langle 3,2\rangle_c$ and $\langle 3,1\rangle_c$ each take care of 50% of the traffic provided by CH $\langle 4,2\rangle_c$. Hence, in slot $T(\langle 4,2\rangle_c)$, CH $\langle 3,1\rangle_c$ is in mode $\mathcal{R}$ in even TDMA frames only and in mode $\mathcal{S}$ in odd TDMA frames[3]. Inversely, CH $\langle 3,2\rangle_c$ is in mode $\mathcal{R}$ in odd and in mode $\mathcal{S}$ in even TDMA frames.

This approach can be generalized to arbitrary rings and sectors. The result is shown in Table II. Remember that the arguments of function $T(x,y)$ in the second column refer to the *sending* CH's cell coordinates. The third column specifies, in dependence of the receiving CH's cell coordinate, the percentage p of frames it actually needs to switch to mode $\mathcal{R}$ in the TDMA slot given in the second column.

TABLE II
RECEPTION SLOTS FOR INBOUND TRAFFIC

	Reception Slots $R(\langle x,y\rangle_c)$ =	Percentage p
A_0	$T(\langle x,-1\rangle_c)$	$1/2x_c$
	$T(\langle x+1,0\rangle_c)$	1
	$T(\langle x+1,1\rangle_c)$	$1/2x_c$
S_0	$T(\langle x+1,y\rangle_c)$	$[2(x_c-y_c)+1]/2x_c$
	$T(\langle x+1,y+1\rangle_c)$	$(2y_c+1)/2x_c$
A_1	$T(\langle x+1,x\rangle_c)$	$1/2x_c = 1/2y_c$
	$T(\langle x+1,x+1\rangle_c)$	1
	$T(\langle x,x+1\rangle_c)$	$1/2x_c = 1/2y_c$
S_1	$T(\langle x+1,y+1\rangle_c)$	$(2x_c+1)/2y_c$
	$T(\langle x,y+1\rangle_c)$	$[2(y_c-x_c)+1]/2y_c$
A_2	$T(\langle 1,y+1\rangle_c)$	$1/2y_c$
	$T(\langle 0,y+1\rangle_c)$	1
	$T(\langle -1,y\rangle_c)$	$1/2y_c$
S_2	$T(\langle x,y+1\rangle_c)$	$(2y_c+1)/2(y_c-x_c)$
	$T(\langle x-1,y\rangle_c)$	$(-2x_c+1)/2(y_c-x_c)$
A_3	$T(\langle x,1\rangle_c)$	$-1/2x_c$
	$T(\langle x-1,0\rangle_c)$	1
	$T(\langle x-1,-1\rangle_c)$	$-1/2x_c$
S_3	$T(\langle x-1,y\rangle_c)$	$[2(y_c-x_c)+1]/(-2x_c)$
	$T(\langle x-1,y-1\rangle_c)$	$[-2y_c+1]/(-2x_c)$
A_4	$T(\langle x-1,x\rangle_c)$	$-1/2y_c = -1/2x_c$
	$T(\langle x-1,x-1\rangle_c)$	1
	$T(\langle x,x-1\rangle_c)$	$-1/2y_c = -1/2x_c$
S_4	$T(\langle x-1,y-1\rangle_c)$	$[-2x_c+1]/(-2y_c)$
	$T(\langle x,y-1\rangle_c)$	$[2(x_c-y_c)+1]/(-2y_c)$
A_5	$T(\langle -1,y-1\rangle_c)$	$-1/2y_c$
	$T(\langle 0,y-1\rangle_c)$	1
	$T(\langle 1,y\rangle_c)$	$-1/2y_c$
S_5	$T(\langle x,y-1\rangle_c)$	$(-2y_c+1)/2(x_c-y_c)$
	$T(\langle x+1,y\rangle_c)$	$(2x_c+1)/2(x_c-y_c)$

TABLE III
TRAFFIC LOAD CARRIED PER CELL HEAD DEPENDING ON THE NUMBER OF RINGS r_{MAX} PRESENT IN ADDITION TO RING 0 (SINK).

$r_{\max}$	Ring (# of nodes)							
	0 (1)	1 (6)	2 (12)	3 (18)	4 (24)	5 (30)	6 (36)	7 (42)
1	6+1	1						
2	18+1	3	1					
3	36+1	6	$^5/_2$	1				
4	60+1	10	$^9/_2$	$^7/_3$	1			
5	90+1	15	$^{14}/_2$	$^{12}/_3$	$^9/_4$	1		
6	126+1	21	$^{20}/_2$	$^{18}/_3$	$^{15}/_4$	$^{11}/_5$	1	
7	168+1	28	$^{27}/_2$	$^{25}/_3$	$^{22}/_4$	$^{18}/_5$	$^{13}/_6$	1

IV. SYSTEM MODEL

We now present the model used for evaluation of the proposed protocol, starting with the model of the traffic generated by each cell and its intra-cell communication to the CH.

A. Intra-Cell Traffic Model

For each CH, we assume that at the end of each mini-slot, a (single) data packet is provided by its cell members with probability a. Under the assumption that the arrival process is independent between mini-slot intervals, the number of data packets that are generated per cell during one combi-frame consisting of N_{FS} mini-slots is given by the probability generating function (PGF)

$$L(z) = (az+1-a)^{N_{FS}} .$$

[3]We assume that clockwise inner-ring neighbors always take care of receiving the traffic sent in the first frame.

The mean number of packets generated by all members of a cell during a single combi-frame is then given by $L'(1) = aN_{FS} = a(N_{CS} + N_{TS}N_{MS})$.

B. Intra-Cell and Inter-Cell Traffic Load

Assuming a lossless model, in order to get stable intra-cell communication, we need to provide sufficiently many mini-slots during contention phase, as preliminarily discussed in Sect. III-B, i.e.,

$$\eta L'(1) = \eta a N_{FS} \le N_{CS} \Rightarrow \frac{\eta a}{1-\eta a} N_{TS} \le \frac{N_{CS}}{N_{MS}} ,$$

while $\eta a < 1$ must be fulfilled.

Let us consider a total number of r_{max} rings. Data packets flow downstream from external rings towards to the sink without loss. For any given CH of ring r and due to the load

balancing, Sect. III-D, the average number of data packets transmitted per frame is given by (cf. Table III)

$$\rho_r = \begin{cases} C_2^{r_{max}+1}\dfrac{L'(1)}{N_{MS}} & \text{for ring} \quad r = 1\,, \\ \dfrac{C_2^{r_{max}+1} - C_2^{r}}{r}\dfrac{L'(1)}{N_{MS}} & \text{for rings} \quad 1 < r \le r_{max}\,. \end{cases} \tag{1}$$

In Eq. (1), $C_n^m = \binom{m}{n}$ more compactly denotes the standard combinatorial number (or binomial coefficient). Clearly, we have $1 > \rho_1 > \rho_2 > \ldots > \rho_{r_{max}}$, where the first inequality gives the stability condition of the WSN. That is,

$$\rho_1 = C_2^{r_{max}+1}\frac{L'(1)}{N_{MS}} = C_2^{r_{max}+1}a\Big(\frac{N_{CS}}{N_{MS}} + N_{TS}\Big) < 1\,. \tag{2}$$

Then, taking into account the local stability condition for the contention phase and the stability condition for the TDMA phase in the first ring (Eq. (2)), we get

$$\frac{\eta a}{1-\eta a}N_{TS} \le \frac{N_{CS}}{N_{MS}} = \frac{\rho_1}{aC_2^{r_{max}+1}} - N_{TS}\,. \tag{3}$$

Consequently, a is upper bounded by

$$a \le \frac{\rho_1}{C_2^{r_{max}+1}N_{TS} + \eta\rho_1} < \frac{1}{\eta}\,, \tag{4}$$

and when a reaches its maximum value, from Eq. (3) we get

$$\frac{N_{CS}}{N_{MS}} = \frac{\eta\rho_1}{C_2^{r_{max}+1}}\,. \tag{5}$$

Hence, for a given coverage area of the WSN expressed in a maximum number of rings r_{max}, for cluster size N_c, for contention factor η, and for a maximum traffic load ρ_1 in CHs of ring 1, we derive the parameter a, the maximum traffic provided individually by each cell. For instance, if $r_{max} = 4$, $N_c = 12$, $\eta = 5$, and $\rho_1 = 0.8$, we get $a \le 1/155$ from Eq. (4). If $a = 1/155$, then $N_{CS}/N_{MS} = 2/5$ according to Eq. (5).

C. Embedded Markov Chain

We assume that each CH has a buffer of infinite capacity. We observe a given CH at the beginning of a $\mathcal{T}$-slot. Let us denote by $F(z) = \sum_{i=0}^{\infty} f_i z^i$ the PGF of the number of packets that arrive to the tagged CH during a combi-frame of duration T_{CF}. The instants at which the $\mathcal{T}$-slots start define an embedded Markov chain which is characterized by the stochastic matrix (given for $N_{MS} = 2$)

$$\boldsymbol{P} = \begin{bmatrix} f_0 & f_1 & f_2 & f_3 & \cdots \\ f_0 & f_1 & f_2 & f_3 & \cdots \\ f_0 & f_1 & f_2 & f_3 & \cdots \\ 0 & f_0 & f_1 & f_2 & \cdots \\ 0 & 0 & f_0 & f_1 & \cdots \\ \vdots & \vdots & \vdots & \vdots & \ddots \end{bmatrix}.$$

With $\boldsymbol{\pi} = [\pi_0, \pi_1, \pi_2, \ldots]$ the steady state stochastic vector and $\boldsymbol{\pi} = \boldsymbol{\pi}\boldsymbol{P}$, we can write the corresponding set of equations

$$\pi_k = \sum_{i=0}^{N_{MS}-1}\pi_i f_k + \sum_{i=N_{MS}}^{N_{MS}+k}\pi_i f_{N_{MS}+k-i}\,, \quad k = 0, 1, 2, \ldots$$

The PGF of the steady state probabilities, $\pi(z)$, is given by

$$\pi(z) = \sum_{k=0}^{\infty}\pi_k z^k = \frac{\sum_{i=0}^{N_{MS}-1}(z^{N_{MS}} - z^i)\pi_i}{z^{N_{MS}} - F(z)}F(z)\,. \tag{6}$$

From Rouché's theorem (see [17]), the denominator of Eq. (6), $z^{N_{MS}} - F(z)$, has exactly N_{MS} roots in $|z| \le 1$. Since Eq. (6) must be analytical in $|z| \le 1$, the roots in the denominator of Eq. (6) must also be roots in the numerator of Eq. (6). Let us denote these roots by $\hat{r}_0 = 1, \hat{r}_1, \hat{r}_2, \ldots, \hat{r}_{N_{MS}-1}$, i.e., $\hat{r}_i^{N_{MS}} - F(\hat{r}_i) = 0$, for $i = 0, 1, \ldots, N_{MS} - 1$. Then, we can obtain the set of probabilities $\pi_0, \pi_1, \ldots, \pi_{N_{MS}-1}$ by solving the following system of N_{MS} linear equations:

$$\sum_{i=0}^{N_{MS}-1}(N_{MS}-i)\pi_i = N_{MS} - F'(z)_{/z=1} = N_{MS} - F'(1) > 0\,,$$
$$\sum_{i=0}^{N_{MS}-1}(\hat{r}_k^{N_{MS}} - \hat{r}_k^i)\pi_i = 0; \quad k = 1, 2, \ldots, N_{MS} - 1\,,$$

where the first equation is based on $\lim_{z\to 1}\pi(z) = 1$ (l'Hopital rule) and the inequality is due to the stability condition. The moments of the random variable (number of data packets that are located at the CH at the beginning of the $\mathcal{T}$-slot) can be obtained by taking successive derivatives of Eq. (6).

D. Some Aspects of the Output Process

According to the CH's behavior described in Sect. III-C, the number of customers served during one time slot is a random variable with PGF given by

$$D(z) = \sum_{i=0}^{N_{MS}} d_i z^i = z^{N_{MS}} - \sum_{i=0}^{N_{MS}-1}\pi_i\big(z^{N_{MS}} - z^i\big)\,, \tag{7}$$

with first and second moments given by

$$\begin{aligned} D'(1) &= N_{MS} - \sum_{i=0}^{N_{MS}-1}\pi_i\big(N_{MS} - i\big) = F'(1)\,, \\ D''(1) &= N_{MS}(N_{MS}-1) \\ &\quad - \sum_{i=0}^{N_{MS}-1}\pi_i\big[N_{MS}(N_{MS}-1) - i(i-1)\big]\,. \end{aligned} \tag{8}$$

In Eq. (8), the last equality comes from the fact that in equilibrium the service rate per combi-frame equals to the arrival rate per combi-frame. Then, the average number of packets found at the beginning of a $\mathcal{T}$-slot can be written as, after some simple algebra,

$$\pi'(1) = F'(1) + \frac{F''(1) - D''(1)}{2[N_{MS} - F'(1)]}\,.$$

E. Detailed Frame Structure

For solving Eq. (6), we need to quantify $F(z)$. For tractability reasons and without loss of generality we assume that all frames start with a $\mathcal{T}$-slot, i.e., the slot label "0" is assigned to the $\mathcal{T}$-slot.

Recalling the combi-frame structure (Fig. 2) and neglecting the synchronization period, we see that there are $1 + N_{TS}$ intervals in a combi-frame: one single interval for the contention period (in the following called $\mathcal{C}$-slot) and $N_{TS} = N_c$ $\mathcal{T}$-slots in the TDMA period. Also, note that the order of intervals depend on the CH we are considering, i.e., different CHs do not necessarily show the same mode pattern. For example, if $r_{max} = 4$ and $N_c = 12$, we get patterns

$[\mathcal{TSSSSSSSCSSSS}]$ for CH $\langle 4,4\rangle_c$,
$[\mathcal{TSSSSSSSSSSCS}]$ for CH $\langle 4,3\rangle_c$,
$[\mathcal{TCSRRSRSSSSSS}]$ for CH $\langle 3,3\rangle_c$, and
$[\mathcal{TSCRRSSSSSSSS}]$ for CH $\langle 3,2\rangle_c$.

Assuming independence of the arrival process between non-overlapping intervals and denoting by $A_i(z)$ the PGF of the number of arrivals during interval i, $i = 0, 1, \ldots, N_{TS}$, we have

$$F(z) = \prod_{i=0}^{N_{TS}} A_i(z), \quad \text{with } A_i(z) = \begin{cases} L(z) & \text{if } i \in \mathcal{C}\,, \\ R_i(z) & \text{if } i \in \mathcal{R}\,, \\ 1 & \text{if } i \in \mathcal{S}, \mathcal{T}\,, \end{cases}$$

with $R_i(z) = p\hat{D}(z) + (1-p)$, where $\hat{D}(z)$ denotes the PGF of the corresponding outer-ring neighbor's output process (Eq. (7)) and p is the percentage of traffic actually received by the tagged CH as given in Table II.

V. Delay and Energy Measures

In this section, we derive the quantitative delay, energy, and combined cost measures based on the proposed model. The measures are used in Sect. VI for evaluating the proposed protocol in an example WSN scenario.

A. Packet Delay

For each CH under study, let us denote by $\overline{b}_i$ the mean number of data packets stored at the beginning of time interval i ($i = 0, 1, \ldots, N_{TS} = N_c$), expressed as

$$\overline{b}_i = \begin{cases} \pi'(1) & \text{for } i = 0\,, \\ \pi'(1) - D'(1) + \sum_{j=0}^{i-1} A'_j(1) & \text{for } i = 1, 2, \ldots, N_{TS}+1\,. \end{cases} \tag{9}$$

Notice that for $i = N_{TS}+1$, in the second equation of Eq. (9), we get $\overline{b}_{N_{TS}+1} = \pi'(1) - D'(1) + F'(1) = \overline{b}_0$. Now we define $Z_i = N_{MS}$ if $i \in \mathcal{R}$, $\mathcal{S}$, $\mathcal{T}$ and $Z_i = N_{CS}$ if $i \in \mathcal{C}$, to approximate the mean number of data packets in the CH by

$$\overline{N_p} = \frac{\sum_{i=0}^{N_{TS}} Z_i \overline{b}_i}{N_{CS} + N_{MS}N_{TS}} = \pi'(1) - D'(1) + \frac{\sum_{k=0}^{N_{TS}} Z_k \sum_{j=0}^{k} A'_j(1)}{N_{CS} + N_{MS}N_{TS}}\,.$$

For an arbitrary data packet, the per-hop delay (mean sojourn time (waiting + service) in a given CH) expressed in combi-frames, can be estimated as (Little formula)

$$\overline{W}_p = \frac{\overline{N_p}}{D'(1)} = \\ = \frac{F''(1) - D''(1)}{2D'(1)[N_{MS} - F'(1)]} + \frac{\sum_{k=0}^{N_{TS}} Z_k \sum_{j=0}^{k} A'_j(1)}{D'(1)(N_{CS} + N_{MS}N_{TS})}\,. \tag{10}$$

B. Energy Consumption Due to Packet Storage

In the mean, a data packet is present at the CH during sojourn time $\overline{W}_p$ given by Eq. (10). The energy (in joule, J) consumed by the packet during its visit is given by $C_H \times \overline{W}_p$, where C_H is a hardware parameter that defines the electric power (in watt, W) needed to store a packet. Since $D'(1)$ is the data arrival rate (packets per frame), the total energy consumption (in W) due to packet buffering is expressed as (normalized to T_{MS}, the duration of a mini-slot and single data packet transmission)

$$\begin{aligned} F_{\text{Stor}} &= D'(1) C_H \overline{W}_p (N_{CS} + N_{MS}N_{TS}) \\ &= C_H \overline{N}_p (N_{CS} + N_{MS}N_{TS})\,. \end{aligned} \tag{11}$$

C. Energy Cost Due to Mode Operation

The measure of energy consumption also needs to take into account the energy consumed by operation in modes[4] $\mathcal{C}$, $\mathcal{R}$, $\mathcal{S}$, and $\mathcal{T}$ and by switching between these modes (for the latter see Sect. V-D). Let us define C_C, C_R, C_S, and C_T as the energy consumption (in W) for a node being in modes $\mathcal{C}$, $\mathcal{R}$, $\mathcal{S}$, and $\mathcal{T}$, respectively. For a given CH, we have N_{CS} mini-slots allocated to the contention phase $\mathcal{C}$. For the other $N_{MS}N_{TS}$ mini-slots of the frame, we consider the traffic load managed by the CH in modes $\mathcal{R}$ and $\mathcal{T}$. Then, for any node that belongs to ring k = 1, 2, ..., r_{max}, the average numbers of mini-slots used in each mode are given by

$$\begin{aligned} N_C &= N_{CS} \quad \text{in mode } \mathcal{C}\,, \\ N_T &= \rho_k N_{MS} \quad \text{in mode } \mathcal{T}\,, \\ N_R &= \frac{C_2^{r_{max}+1} - C_2^{k+1}}{C_2^{r_{max}+1} - C_2^{k}} \rho_k N_{MS} \quad \text{in mode } \mathcal{R}\,, \\ N_S &= N_{MS}N_{TS} - N_T - N_R \quad \text{in mode } \mathcal{S}\,. \end{aligned}$$

The energy cost (in W) for operating in all modes is then

$$F_{\text{Oper}} = \frac{\sum_{i \in C,R,S,T} C_i N_i}{N_{CS} + N_{MS}N_{TS}}\,. \tag{12}$$

D. Energy Cost Due to Mode Switching

Let $C_{\overrightarrow{SC}}$, $C_{\overrightarrow{SR}}$, and $C_{\overrightarrow{ST}}$ be the energy consumption (in in J/(Switches × Mean Service Time), i.e., in W) caused by switching from mode $\mathcal{S}$, to modes $\mathcal{C}$, $\mathcal{R}$ and $\mathcal{T}$, respectively. Note that switching from modes $\mathcal{C}$, $\mathcal{R}$ and $\mathcal{T}$ to mode $\mathcal{S}$ usually does not consume significant energy, so $C_{\overrightarrow{CS}} \approx C_{\overrightarrow{RS}} \approx C_{\overrightarrow{TS}} \approx 0$. Then, we have to account for the number of visits to a given mode ($\mathcal{C}$, $\mathcal{R}$, or $\mathcal{T}$) per combi-frame:

$SW_C = 1$ visit to mode $\mathcal{C}$,
$SW_R = 2$ visits to mode $\mathcal{R}$ if the CH $\in S_k$, $k = 0, \ldots, 5$,
$SW_R = 3$ visits to mode $\mathcal{R}$ if the CH $\in A_k$, $k = 0, \ldots, 5$,
$SW_T = 1$ visit to mode $\mathcal{T}$.

[4]Mode $\mathcal{C}$ summarizes the execution of $\mathcal{R}$, $\mathcal{S}$, and $\mathcal{T}$ modes during contention phase.

Consequently, the switching energy cost (in W) is

$$F_{\text{Switch}} = \frac{\sum_{i \in C,R,T} C_{\overrightarrow{Si}} SW_i}{N_{CS} + N_{MS} N_{TS}} . \quad (13)$$

E. Total Energy Cost

For each node, the total energy consumption is given by the sum of the storage cost (Eq. (11)), the operation mode cost (Eq. (12)), and the switching cost (Eq. (13)). For a fixed cluster size N_{TS}, notice that Eq. (11) increases with N_{MS}, Eq. (12) stays constant (because N_{NC}/N_{MS} is constant according to Eq. (3)), and Eq. (13) decreases with N_{MS}. Then, the total energy cost (in W) is given by

$$C_E = F_{\text{Stor}} + F_{\text{Oper}} + F_{\text{Switch}} . \quad (14)$$

F. Total Cost

We define a dimensionless total cost as the weighted sum of the delay (Eq. (10)) and energy (Eq. (14)) costs, where $0 \le \alpha \le 1$ is the weighting factor, i.e.,

$$C(\alpha) = (1-\alpha)\frac{\overline{W}_p}{\text{s}} + \alpha \frac{C_E}{\text{W}} , \quad (15)$$

where s and W refer to the units *combi-frames* and *watt*, respectively. If the energy consumption is of high importance, we choose α close to one. In contrast, when α is small, high importance is given to the delay. Note that while $C(\alpha)$ has no effective interpretation in the physical world, it helps to qualitatively investigate the delay versus energy efficiency trade-off.

VI. Investigation of 4-Ring WSN

We investigate the nodes of a 4-ring WSN with a total utilization of $\rho_1 = 0.8$ at ring-1 nodes (see Eq. (1)). According to Table III, the utilizations for rings 2, 3, and 4 are then 0.36, $0.18\bar{6}$, and 0.08, respectively. For $\rho_1 = 0.8$, for a contention factor equal to $\eta = 5$ and for a number of TDMA slots $N_{TS} = 12$, we get from Eq. (4) $a \le 1/155$. When $a = 1/155$ from Eq. (5) we have $N_{CS}/N_{MS} = 2/5$. We now obtain[5] illustrative results for N_{MS}= 5, 10, 15, 20, 25 and 30 while keeping constant the ratio $N_{CS}/N_{MS} = 2/5$.

The parameters of Eqs. (11), (12), and (13) are chosen as follows. For C_H in Eq. (11) we consider $C_H = 0.2\,\text{W}$, quite in parallel to the values provided in [18]. For operation modes $\mathcal{C}$, $\mathcal{R}$, $\mathcal{S}$, and $\mathcal{T}$, we consider the Mica2 mote (see [19]) as reflected in Table IV. For mode $\mathcal{S}$, we choose $C_S = 36\,\text{mW}$ (microprocessor is on, transceiver is off). For modes $\mathcal{C}$ and $\mathcal{R}$, we chose $C_C = C_R = 66\,\text{mW}$, and for mode $\mathcal{T}$, $C_T = 141\,\text{mW}$. When switching from sleeping mode $\mathcal{S}$ to modes $\mathcal{C}$, $\mathcal{R}$, or $\mathcal{T}$, we take into account that the power supply's voltage is 3 V, the absorbed current is 15 mA, and the transition time is 250 μs, which gives a total amount of 11.25 μJ. Assuming a service time per data packet equal to 2×10^{-3} seconds, we get a switching power consumption of approximately 5.63 mW (normalized to the service time). Therefore, we have for operation modes $C_S = 36\,\text{mW}$, $C_C = C_R = 66\,\text{mW}$, and $C_T = 141\,\text{mW}$, and for switching modes $C_{\overrightarrow{SC}} = C_{\overrightarrow{SR}} = C_{\overrightarrow{ST}} = 5.63\,\text{mW}$. For the parameter α of Eq. (15), we chose values $\alpha = 0.2$ and $\alpha = 0.8$, to give some preference to energy consumption over the delay and vice-versa, respectively.

[5]Evaluation of the queueing model requires localization of the roots of $z^{N_{MS}} - F(z)$, Eq. (6), a polynomial with maximum degree, equal to $3N_{MS} + (N_{CS} + N_{TS}N_{MS})$ for CHs $\in \{A_0 \ldots A_5\}$ and equal to $2N_{MS} + (N_{CS} + N_{TS}N_{MS})$ for CHs $\in \{S_0 \ldots S_5\}$. Consequently, with the given values and for $N_{MS} = 25$, in the first case we have to find 385 roots, 25 out of them with modulus less than or equal to 1.

TABLE IV
Energy Consumption of MICA2 Motes (in mW)

Operation modes				Mode switching		
C_S	C_C	C_R	C_T	$C_{\overrightarrow{SC}}$	$C_{\overrightarrow{SR}}$	$C_{\overrightarrow{ST}}$
36	66	66	117–165	5.65	5.65	5.65

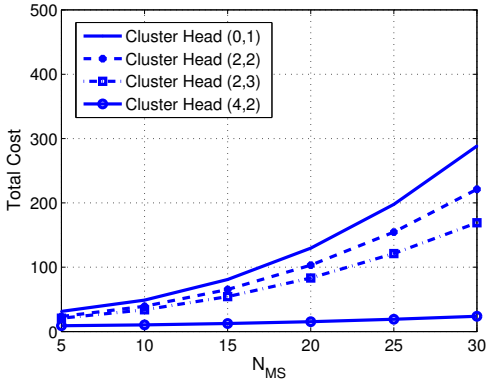

Fig. 4. Total cost of four CHs located in rings 1 to 4 for $\alpha = 0.2$.

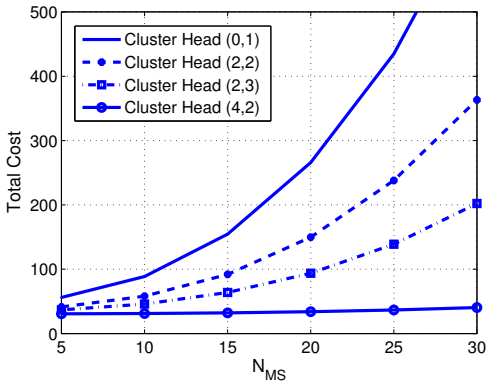

Fig. 5. Total cost of four CHs located in rings 1 to 4 for $\alpha = 0.8$.

In Figs. 4 and 5, we show the total costs given by Eq. (15) of CH $\langle 0,1 \rangle_c$ (ring 1), $\langle 2,2 \rangle_c$ (ring 2), $\langle 2,3 \rangle_c$ (ring 3), and $\langle 4,2 \rangle_c$ (ring 4). In Fig. 4 with $\alpha = 0.2$, we give more importance to the delay. In Fig. 5 with $\alpha = 0.8$, we give more importance to the energy consumption. In both cases, it is clear that CHs close to the sink consume more energy than CHs far from the sink, as it could be expected. Secondly, TDMA frames with minimum length (smallest N_{MS}) are more efficient than larger frames, mainly due to the fact that the cost induced by packet

storage has greater effect than the mode switching costs. Note that the cost due to the operation mode remains constant when N_{MS} varies while the traffic load ρ_k and the ratio N_{CS}/N_{MS} remain constants, see Eq. (12).

VII. Conclusions

In this work, we study the trade-off between energy consumption and delay in WSNs while also taking medium access control into account. To mitigate the energy hole problem we provide a routing procedure that forwards the data packets such that a balancing of energy consumption is guaranteed. A discrete-time Markov model is defined that deals with the TDMA protocol for inter-cell communication. The model reflects the contention, reception, sleeping, and transmission modes of the cells' head nodes and considers the data traffic being forwarded to the sink node. The final model is used to capture the energy consumption due to the frequency of mode switching, the energy cost associated to each operation mode, and the energy consumed by data packets waiting in the buffer of each cell head. Results show a convex weighted cost function that allows to determine the optimal frame duration and consequently the number of mini-slots N_{MS} per frame.

Our paper shows that our approach allows significant optimization, and hence, it is worthwhile to invest further effort in more detailed and more complex investigation. In particular, we plan to include a more detailed contention model, which is able to calibrate the contention process in the intra-cell communications, into the study, to quantify in a precise manner the contention parameter η. Additionally, we aim at including consideration of other reuse patterns for reuse slots, in a parallel way to mobile cellular scenarios. In particular, the combi-frame proposed in Fig. 2 could be optimized by using unused TDMA slots for intra-cluster communication, i.e., when the cell head is in sleeping mode. For example, in a scenario with cluster size greater than 12, some TDMA slots could be used for intra-cell communication without interfering with inter-cell communication processes in progress within the same and adjacent clusters. Alternatively, replacing the contention phase by a second TDMA phase with smaller cluster size might be advantageous for controlling high-load inter-cell traffic. We are planning to compare these protocol variants using extensions to the model presented in this paper. Further studies also include looking at unreliable nodes. This implies need for acknowledgments and/or using alternative routes to the sink. Consequently, our model needs to be transferred from the current feed-forward type to a queueing network with feedback. Further options of generalizing the model include tackling irregular placement of cell heads. Moreover, simulations for real scenarios are necessary in order to validate the presented and future results.

Acknowledgment

All the authors thank for the support received from the Network of Excellence Euro-NF (FP7, IST 216366). Universitat Politècnica de València is partly supported by the Spanish national project TIN2010-21378-C02-02. University of Passau is partly supported by the SOCIONICAL project (FP7-ICT-2007-3, Grant No. 231288) and by the Network of Excellence EINS (FP7-ICT-2011-7, Grant No. 288021).

References

[1] J. L. Hammond and P. J. P. O'Reilly, *Performance Analysis of Local Computer Networks*. Addison-Wesley Publishing Company, 1986.

[2] L. Shi and A. O. Fapojuwo, "TDMA scheduling with optimized energy efficiency and minimum delay in clustered wireless sensor networks," *IEEE Transactions on Mobile Computing*, vol. 9, no. 7, pp. 927–940, July 2010.

[3] J. K. Murthy, S. Kumar, and A. Srinivas, "Energy efficient scheduling in cross layer optimized clustered wireless sensor networks," *Int'l Journal of Computer Science and Communication*, vol. 3, no. 1, pp. 149–153, 2012.

[4] I. F. Akyildiz and M. C. Vuran, *Wireless Sensor Networks*. John Wiley & Sons, July 2010.

[5] V. Turau, C. Weyer, and C. Renner, "Efficient slot assignment for the many-to-one routing pattern in sensor networks," in *Proc. of the 1st Int'l Workshop on Sensor Network Engineering (IWSNE 2008)*, June 2008.

[6] E. Martin, L. Liu, M. Covington, P. Pesti, and M. Weber, *Location-Based Services Handbook – Applications, Technologies, and Security*. CRC Press, 2010, ch. Positioning Technologies in Location-Based Services, pp. 1–45.

[7] A. Pal, "Localization algorithms in wireless sensor networks: Current approaches and future challenges," *Network Protocols and Algorithms*, vol. 2, no. 1, pp. 45–74, 2010.

[8] L. M. Pestana Leão de Brito and L. M. Rodríguez Peralta, "An analysis of localization problems and solutions in wireless sensor networks," *Tékhne - Revista de Estudos Politécnicos*, vol. 6, no. 9, pp. 1–27, 2008.

[9] A. C. Pinho, D. R. Figueiredo, and F. M. G. Franca, "A robust gradient clock synchronization algorithm for wireless sensor networks," in *Proc. of 4th Int'l Conf. on Communication Systems and Networks (COMSNETS 2012)*, January 2012, pp. 1–10.

[10] Y. Xu, J. Heidemann, and D. Estrin, "Geography-informed energy conservation for ad hoc routing," in *Proc. of the 7th ACM annual Int'l Conf. on Mobile computing and networking (MOBICOM 2001)*. ACM, 2001, pp. 70–84.

[11] V. H. MacDonald, "Advanced mobile phone service: The cellular concept," *Bell System Technical Journal*, vol. 58, no. 1, pp. 15–41, January 1979.

[12] H. Ando, E. Kulla, L. Barolli, A. Durresi, F. Xhafa, and A. Koyama, "A new fuzzy-based cluster-head selection system for WSNs," in *Int'l Conf. on Complex, Intelligent and Software Intensive Systems (CISIS 2011)*, July 2011, pp. 432–437.

[13] A. Pires, C. Silva, E. Cerqueira, D. Monteiro, and R. Viegas, "CHEATS: A cluster-head election algorithm for WSN using a Takagi-Sugeno fuzzy system," in *Proc. of IEEE Latin-American Conf. on Communications (LATINCOM 2011)*, October 2011, pp. 1–6.

[14] H. Taheri, P. Neamatollahi, M. Yaghmaee, and M. Naghibzadeh, "A local cluster head election algorithm in wireless sensor networks," in *Proc. of CSI Int'l Symposium on Computer Science and Software Engineering (CSSE 2011)*, June 2011, pp. 38–43.

[15] R. Rom and M. Sidi, *Multiple access protocols – performance and analysis*. Springer Verlag, 1990.

[16] J. Mosely and P. A. Humblet, "A class of efficient contention resolution algorithms for multiple access channels," *IEEE Transactions on Communications*, vol. 33, no. 2, pp. 145–151, 1985.

[17] I. Adan, J. van Leeuwaarden, and E. Winands, "On the application of Rouché's theorem in queueing theory," *Operations Research Letters*, vol. 34, pp. 355–360, 2006.

[18] F.-C. Jiang, H.-W. Wu, D.-C. Huang, and C.-H. Lin, "Lifetime security improvement in wireless sensor network using queue-based techniques," in *Proc. of the Int'l Conf. on Broadband, Wireless Computing, Communication and Applications*, 2010.

[19] R. Maheswar and R. Jayaparvathy, "Performance analysis of cluster based sensor networks using N-policy M/G/1 queueing model," *Eur. J. Scientific Research*, vol. 58, no. 2, pp. 177–188, August 2011.